The polythiophene molecular segment as a sensor model for H_2O, HCN, NH_3, SO_3, and H_2S: A Density Functional Theory study

Ali Shokuhi Rad [1]*, Mehri Esfahanian [1], Etesam Ganjian [2], Habib-allahTayebi [3], Samaneh Bagheri Novir [4]

[1]Department of Chemical Engineering, Qaemshahr Branch, Islamic Azad University, Qaemshahr, Iran

[2] Department of Chemical Engineering, Babol Noshirvani University of technology, Babol, Iran

[3]Department of Textile Engineering, Qaemshahr Branch, Islamic Azad University, Qaemshahr, Iran

Department of Chemistry, Pharmaceutical Sciences Branch, Islamic Azad University, Tehran, Iran

*E-mail: *a.shokuhi@gmail.com*, *a.shokuhi@qaemshahriau.ac.ir*

Tel: 0098-9112134588

Fax: 0098-11132367735

Abstract

Study of the interaction of some atmospheric gases (H_2O, HCN, NH_3, SO_3 and H_2S) with an oligomer (3PT) is important because of developing polymeric sensor for gas detection. In the following, we focused on the relaxed geometries, interaction energies, charge analysis, HOMO-LUMO orbital analysis, and UV-vis study of all interacted systems using first-principles density functional theory (DFT). All these analysis show the possibility of polythiophene as an inexpensive polymeric sensor towards mentioned analytes. The values of interaction energy were achieved as -19.90, -19.66, -14.01, -8.70, and -4.76 kJ/mole for adsorption of SO_3, H_2O, NH_3, HCN, and H_2S on 3PT, respectively. Consequently the clarification of their physical parameters is the major target of this study.

Keywords: Polythiophene, DFT, adsorption, polymeric sensor, molecular interaction

1. Introduction

Conductive polymers are well-known because of their electronic as well as physical properties [1]. In comparison with the inorganic semiconductors, they have many advantages such as straightforward synthesis and processing. Their electronic properties are specified by the π- π electrons transferring between carbon backbones [2]. Polymeric gas sensors have received great attentions as candidate for inexpensive sensor applications [3, 4]. Based on our findings, poly (3,4-ethylenedioxythiophene), polyaniline, polypyrrole and poly(o-phenylenediamine) are extensively studied as biosensors and gas sensors [3]. Beside the development of gas sensor, the principal goal of molecular modeling is to provide theoretical support to find the potential of sensor. First-principle modeling gives significant physical properties without the use of experimental information [5-18]. As an example, in our previous work, we used density functional theory calculations to investigate the response mechanism of polypyrrole as a gas sensor towards detection of SO_2, NH_3, H_2O, CO, CH_4 and CO_2 [8]. We found high capability of this sensor for detection of H_2O and NH_3 molecules. In another work [9] we used DFT calculation to principles study of terpyrrole as a sensor for hydrogen cyanide.

Among all conducting polymers, polythiophene (Scheme 1) and its derivatives are famous because of their low cost, easy process and high thermal stability for different purpose such as electromagnetic shielding and molecular electronic. In our previous work we focused on the sensing property of terthiophene towards SO_2 and SO_3 species using DFT at B3LYP/6-31+G(d) level of theory and then the results were compared with M06-2X/6-functional at the same basis set [10]. We found significant interaction between SOx and terthiophene as a model of polythiophene.

There are several studies which focused on the electronic structure of different thiophenes [19, 20]. For example, Bouzzine et al. [21] studied on the polythiophene energy band gap and the effects of its substitutions. There are some successfully applications of polythiophene as gas sensor. For example Liao et al. [22] used X-ray reflectivity study on polythiophene and showed in situ characterization of the physical interaction between the analyte molecules and the polythiophene films. For this purpose, they used this sensor for amine (Butylamine) and found that, there is a small change in the film thickness upon exposure to the analytes.

Sakurai et al. [23] used polythiophene and its derivatives as polymeric sensors towards odor gases such as NH_3, $CHCL_3$, CH_4, iso-butane and ethanol. Based on their study, the response behavior of polythiophene was detected as the altering in the resistance against analytes. They found that NH_3 has maximum of sensitivity among studied species. On exposure to NH_3, the resistance of polythiophene film suddenly increased and then remained steady when NH_3 was replaced by air.

There are different principles or transduction techniques for gas detection of polythiophene (and other related polymers), such as optical absorption (for example, application of UV-vis analysis), and the conductivity which is based on measuring the change in the conductivity of polymer upon adsorption of different analytes. Both principles performed experimently by Concalves et al. [24, 25]. They used active layer of the polythiophene derivative as a sensor and analyzed its conductivity as response for contact to dynamic flow of saturated vapors of six volatile organic compounds [24]. They received different responses upon adsorption of different analytes.

In parallel to conductivity measurement, Optical measurement is another suitable method for remote detection and offers large usefulness at low cost. As an example, Goncalves et al. [25] in another research, reported the use of thin films of some polythiophene derivatives as active layer in optical sensors for the detection of six volatile organic compounds. They found that

differentiation could be executed based on the presence or not of response to an analyte and the sensitivity value of the sensors for the analytes.

Based on the above-mentioned examples of polythiophene's application as sensor for different analytes, it seems that the study of specie-polythiophene interaction will be important to distinguishing how the electronic structure of polymer could be changed upon adsorption of different analytes.

To fully developing of a sensor, it is essential to recognize the kind of interaction between sensor and analytes. The interaction of different analytes on polythiophene (as gas sensor) changes its electronic structure, which results an alteration in the electric conductance of polymer. Furthermore this alteration can be transformed to a signal.

To the best of our knowledge, there is no study on simultaneous interaction of H_2O, HCN, NH_3, SO_3 and H_2S on polythiophene in the literatures, so the main target of this study is to have a conceptual understanding of the electronic properties of thiophene oligomer (as a part of polythiophene having three units of thiophene, denoted here as 3PT) as a model of polymeric sensor upon interaction with above-mentioned species. In order to comparing and understanding the relationship between chemical structure of 3PT-analytes and their electronic properties, we examined the geometrical as well as quantum chemical descriptions of 3PT before and after interaction with H_2O, HCN, NH_3, SO_3 and H_2S.

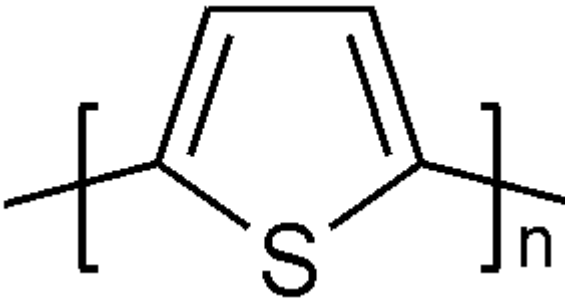

Scheme 1- Polythiophene structure.

.

2- Theoretical method

All geometries were optimized by ORCA 3.0.2 computational package [26] by using DFT method including 6-31+G(d,p) basis set with regarding to applying the BLYP density functional with a version of Grimme's D3 dispersion model [27]. Moreover to have a comparison we used MPW1B95 as additional functional for optimization of all BLYP-D3 relaxed structures. MPW1B95 is one of the well-known functional which gives good performance for hydrogen bonding and weak interaction calculations [28].

The UV–vis spectra of isolated 3PT and 3PT-X complexes were simulated at time-dependant DFT (TD-DFT) using above-mentioned level of theory.

It is well-known that DFT is able to accurately treat such systems because of having the exchange-correlation property [29].

The length of polythiophene was an important choice in our calculations because its size should be as small as possible to saving time and in the other hand, it should have a reliable behavior in practical studies. Our initial calculations reveal that one or two units of thiophene did not show reliable response but three units of thiophene (3PT) showed approximately appropriate and reliable response. Therefore 3PT was chosen and allowed to be optimized based on aforementioned basis set. The edges of 3PT were capped by hydrogen atoms to neutralize the terminal carbons as illustrated in Figure 1(a).

Electronic properties, the energy of lowest unoccupied molecular orbital (E_{LUMO}), the energy of highest occupied molecular orbital (E_{HOMO}), and the band gap (E_g) were calculated at above-mentioned level of theory. The position of the Fermi level (E_{FL}) is just middle of the valence and conduction band and so with approximation it can be achieved by eq 1. [30].

$E_{Fi}= 1/2 (E_{HOMO} + E_{LUMO})$ 1

To calculate the interaction energies of different interactions, the eq.2 has been used. We used counterpoise method to correct this energy based on eq 3. [31].

$E_{int}= E_{3PT-X} - (E_{3PT} + E_X)$ 2

$E_{int, CP} = E_{int} - E_{BSSE}$ 3

where E_{3PT-X} is total energy of the optimized 3PT interacted with different gas molecules, E_{3PT} is total energy of an isolated 3PT, E_X is total energy of any species in the relaxed form, E_{BSSE} is the basis set superposition errors energy for 3PT-X , and finally $E_{int, CP}$ is counterpoise interaction energy of related complexes.

3. Results and discussions

3.1. Geometric parameters

We used Figure 1(a) to show the numbering of the atoms in 3PT during interaction with different analytes for discussing on optimized geometric parameters listed in Table 1.

All relaxed configurations were achieved based on fully optimization of initial position configuration (as input file). We considered two initial configurations for all analytes to be closed to the S atom of thiophene:. for HCN (the H-side and N-side), H_2O (the O-side and H-side), NH_3 (the N-side and H-side), SO_3 (the S-side and O-side), and H_2S (the H-side and S-side). In the case of H_2O, HCN, and H_2S during fully optimization, their two initial positions results unit relaxed structure. In the case of SO_3 and NH_3 there were two relaxed structures resulted by their two initial positions, so we used the more stable one of them (judging from the values of released energy) to furthermore investigation. The fully optimized structures of isolated 3PT and its complexes with H_2O, HCN, NH_3, SO_3 and H_2S are depicted in Figure 1(b-f).

The data of intra-molecular ($d_{S14...X}$) as well as the inter-molecular geometric parameters ($\angle C_5S_{14}C_6$, $\angle C_5S_{14}X$, and dihedral angle ($\angle C_5S_{14}C_6C_9$)) are listed in Table 1. The distance

between 3PT and different analytes ($d_{S14\ldots X}$) changed in order of H_2O<HCN< SO_3<NH_3< H_2S as can be seen from the data listed in Table 1. Highest interaction energy in the case of SO_3 despite to its high distance can be related to its notable orbital hybridizing with 3PT.

Another significant geometric parameter in 3PT and 3PT-X is the angle of bridging ($C_5S_{14}C_6$) which changes when 3PT interacts with different analytes. Considering some exceptional, higher change in this angle normally associates to more interaction energy. This angle increase by H_2O, NH_3, SO_3 and H_2S while decrease by HCN in the order of 3PT-HCN<Isolated 3PT<3PT-H_2S <3PT-NH_3 <3PT-H_2O <3PT-SO_3.

All descriptions about geometric parameters emphasize the exclusive configuration as well as structure of any specie on 3PT which are useful to furthermore investigation on designing polymeric sensor.

The calculated interaction energies of all above-mentioned molecules with 3PT are listed in Table 1. Calculated interaction energies were -19.90 and -21.44 kJ/mole for 3PT-SO_3, -19.66 and -21.34 kJ/mole for 3PT-H_2O, -14.01 and -16.65 kJ/mole for 3PT-NH_3, -8.70 and -10.10 kJ/mole for 3PT-HCN and finally -4.76 and -4.98 kJ/mole for 3PT-H_2S complexes based on functionals of BLYP-D3 and MPW1B95 respectively. It should be mentioned that the values of adsorption energy for 3PT-SO_3 in this present study is quite similar to the values of -22.6 kJ/mole for this system achieved by using B3LYP functional in our previous paper [10].The differences obtained *via* the two distinct functionals are not just acceptable but they give the same qualitative information, which reinforce the robustness of the methodology employed.

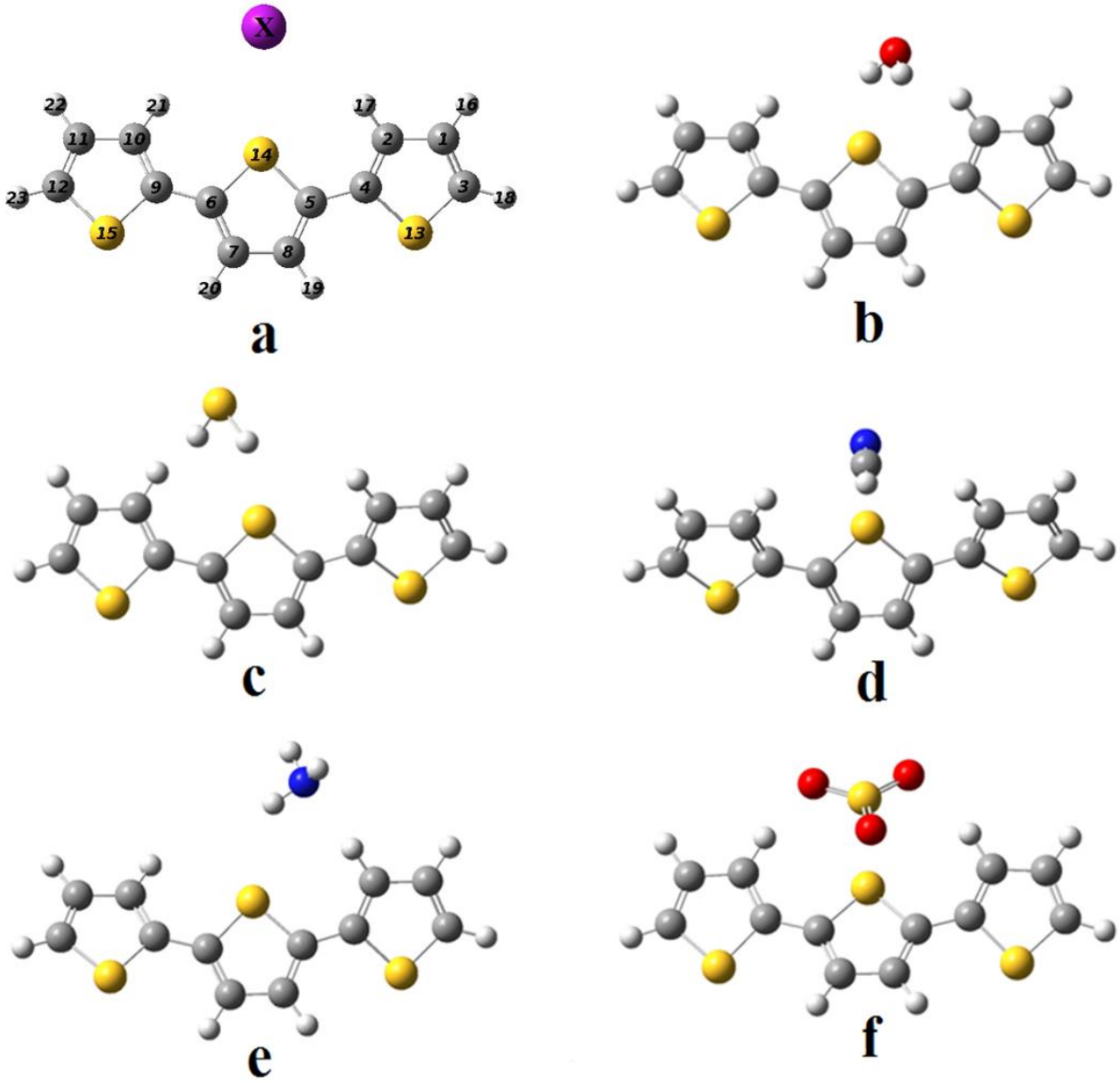

Figure 1. The fully optimized structures of isolated 3PT ((a) X here known as dummy atom as a part of analyte) and its complexes with H_2O (b), H_2S (c), HCN (d), NH_3 (e), and SO_3 (f).

Table 1. Optimized geometric parameters (Bond lengths in A°, bond angles in deg and E_{int} in kJ/mol)

System	Isolated 3PT	3PT-H_2O	3PT-HCN	3PT-NH_3	3PT-SO_3	3PT-H_2S
$d_{S14...X}$[1]	-	2.69	2.82	3.06	3.02	3.08

$\angle C_5S_{14}C_6C_9$	179.78	179.64	179.05	179.18	179.28	179.72
$\angle C_5S_{14}X^1$	-	124.87	92.45	131.26	106.61	115.30
E_{int} (BLYP-D3)[2]	-	-19.66	-8.70	-14.01	-19.90	-4.76
E_{int} (MPW1B95)[2]	-	-21.34	-10.10	-16.65	-21.44	-4.98

[1]X is nearest atom of analyte

[2]counterpoise corrected energy

3.2. Charge Analysis

The quantity of charge transfer between 3PT and any of species were evaluated at the BLYP-D3/6-31+G(d) level of theory. Any of above-mentioned species changes the electronic properties of 3PT during charge transfer. This electronic charge transferring will change the resistance, band gap and λ_{max} of 3PT which in fact determine its sensitivity. Mulliken and NBO charge analysis of all analytes (H_2O, HCN, NH_3, SO_3 and H_2S) after interaction with 3PT are given in Table 2. Complex formations of 3PT-analytes were recognized due to the transferring of electrons from analytes to 3PT for H_2O and NH_3 and reverse transferring (3PT to analytes) for SO_3, H_2S, and HCN as can be seen from the data listed in Table 2.

In 3PT-NH_3 and 3PT-H_2O complexes, NH_3 and H_2O, respectively lose about 0.015 and 0.032 e^- charges to 3PT based on NBO, and 0.025 and 0.028 e^- based on Mulliken charge analysis. In other hand, at 3PT-SO_3, 3PT-H_2S, and 3PT-HCN complexes, SO_3, H_2S and HCN species take 0.068, 0.021 and 0.011 e^- charges from 3PT based on NBO and 0.070, 0.031, and 0.016 e^- based on Mulliken charge analysis, respectively. These are acceptable differences between the results of NBO and Mulliken charge analysis. The results of charge transfer points to this matter of fact that the probe molecules are acting as H-bond donor for H_2S and HCN whereas in other (i.e., H_2O and NH_3), as H-bond acceptor.

It can be seen that highest charge transfer relates to SO_3 which corresponds to its highest interaction energy among all species. Despite to the highest charge transfer for SO_3, this value of charge still is not too big to categorize the interaction in chemisorption region. These low charge values for all interactions are totally in agreement to their relative low interaction energies and are proving for van der Waals interaction.

3.3 Orbital analysis

Figure 2 shows the distributions of HOMO and LUMO for isolated 3PT and complexed forms of species: 3PT-SO_3, 3PT-H_2O, 3PT-NH_3, 3PT-HCN and 3PT-H_2S. As can be seen in Fig. 2, by exception of 3PT-SO_3, for all systems, both HOMO and LUMO are localized on 3PT which is proofing for low interaction. For 3PT-SO_3, the LUMO is mainly located on the SO_3 and on ring 2 of 3PT. This relocation of LUMO corresponds to the highest change in the E_{gap} which results highest interaction energy.

The energy of HOMO and LUMO for isolated 3PT are found to be −5.189 eV, −1.637 eV respectively. An increase of 0.127, 0.263, 0.204 and 0.097 eV of energies are given in the HOMO of 3PT on sensing H_2O, HCN, SO_3, and H_2S respectively. Moreover a decrease of 0.131 eV of energy is simulated in the HOMO of 3PT on sensing NH_3.

The data reveals that the energies of LUMO for 3PT increased after interaction with H_2O, HCN, SO_3 and H_2S while decreased by NH_3. Consequently the HOMO-LUMO energy gap is one of the key parameter to distinguish the electronic stability of resulted interactions. The calculated E_g value for isolated 3PT (3.552 eV) is close to its experimentally measured (3.520 eV) by Diaz et al. [32].

As can be seen in Table 2, the band gap of each analyte is much higher compared to that of 3PT. However upon complexation, the band gap of resulted complex is quite different than that of the isolated 3PT, depending on the nature of analyte. We can say (but not in overall) that if the difference in the band gaps of analyte and adsorbent be shorter, the change in the

band gap of their complex is more considerable (more hybridizing) such as what can be seen for the case of SO_3. For other species such as H_2O the big difference in the E_{gap} of the analyte and 3PT causes insignificant change in the bond gap of resulted complex which makes it difficult to transfer electron [33].

The band gaps of energy for different complexes considering the isolated 3PT are in order of 3PT-SO_3 < Isolated 3PT < 3PT-HCN < 3PT- H_2S < 3PT-NH_3 < 3PT- H_2O. So we can conclude that 3PT-H_2O has the lowest conductivity whereas 3PT-SO_3 has the highest conductivity among all studied species.

The work functional of 3PT sensor can be interpreted by means of calculating the difference in potential energies of the vacuum level and the Fermi level, which is the least amount of required energy for removing one electron from the Fermi level to the vacuum [34]. The change in the value of Fermi level of 3PT upon interaction with different analytes is a mathematical description of saying that there is more electrons (holes) of any complex, in compare with the isolated 3PT. The value of E_{FL} changed from -3.413 eV for isolated 3PT to -3.510, -3.676, -3.269, -4.078 and -3.503 eV for 3PT-H_2O, 3PT-HCN, 3PT-NH_3, 3PT-SO_3 and 3PT-H_2S, respectively.

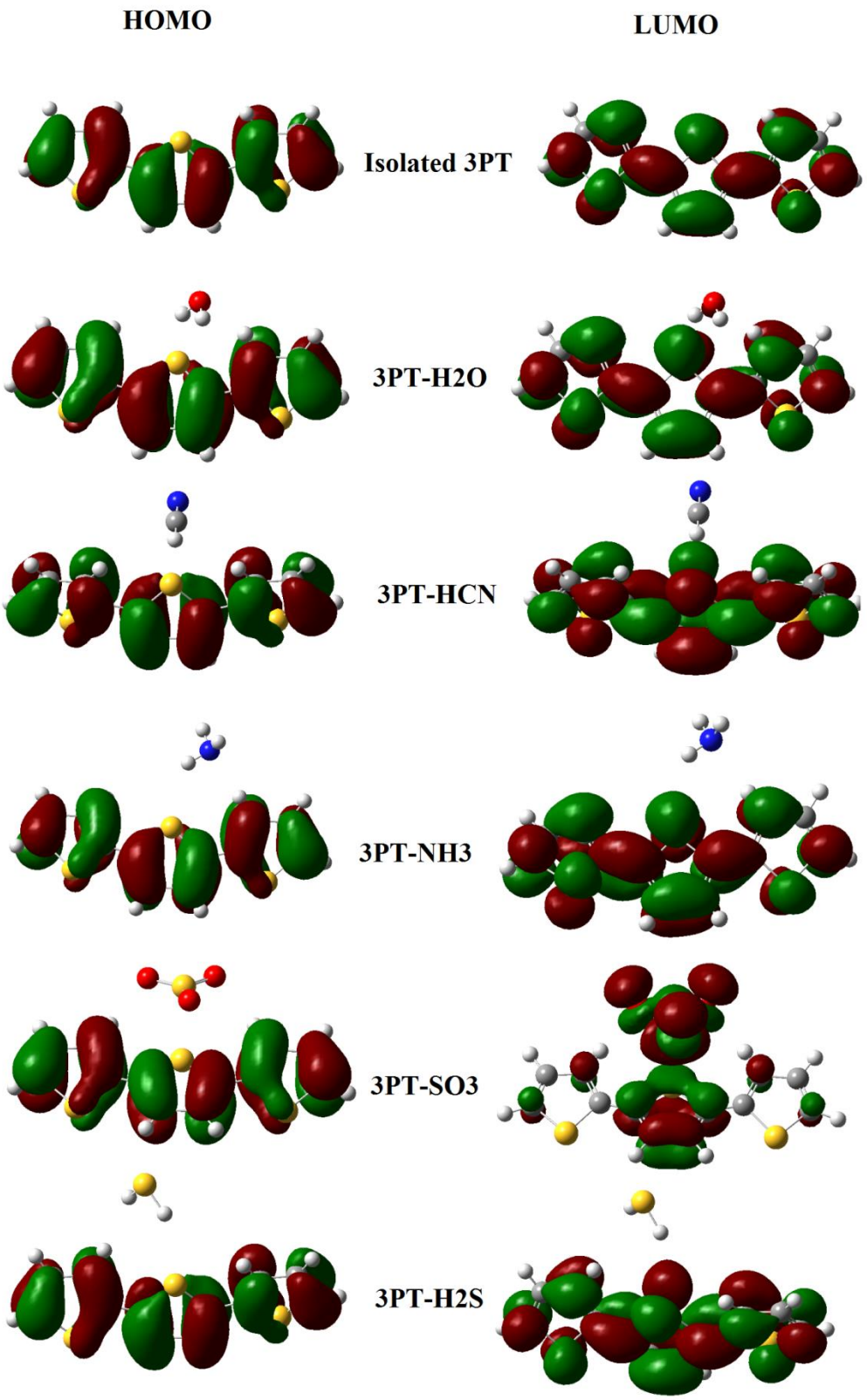

Figure 2. The molecular orbitals of HOMO and LUMO for (top to down): isolated 3PT, 3PT-H_2O, 3PT-HCN, 3PT-NH_3, 3PT-SO_3 and 3PT-H_2S at the BLYP-D3/6-31+G(d) level.

Table 2. The electronic properties of systems: Calculated charge transfer by Mulliken ($Q_{Mulliken}$) and NBO (Q_{NBO}), E_{HOMO}, E_{LUMO}, energy of Fermi level (E_{FL}), and E_g.

System	$Q_{Mulliken}$ (e)	Q_{NBO} (e)	E_{HOMO} (ev)	E_{FL} (ev)	E_{LUMO} (ev)	E_g (ev)
H_2O	-	-	-7.924	-3.110	1.704	9.628
HCN	-	-	-9.771	-4.605	0.561	10.332
NH_3	-	-	-6.868	-2.364	2.139	9.007
SO_3	-	-	-9.459	-6.207	-2.955	6.504
H_2S	-	-	-7.116	-3.290	0.536	7.652
Isolated 3PT	-	-	-5.189	-3.413	-1.637	3.552
3PT- H_2O	+0.028	+0.032	-5.316	-3.510	-1.705	3.611
3PT-HCN	-0.016	-0.011	-5.452	-3.676	-1.891	3.561
3PT-NH_3	+0.025	+0.015	-5.058	-3.269	-1.480	3.578
3PT-SO_3	-0.070	-0.068	-5.393	-4.078	-2.764	2.629
3PT-H_2S	-0.031	-0.021	-5.286	-3.503	-1.720	3.570

3.4. UV-vis spectra

We simulated the UV–vis spectra of both isolated as well as complexed form of 3PT using time-dependant DFT by using BLYP-D3/6-31+G (d) level of theory. Figure 3 shows the spectra and Table 3 presents the main peak positions and information regarding the observed shifts. The experimental λ_{max} value of nPT is about 440 nm (2.82 eV) [35], which is 0.52 eV lower than our calculated λ_{max} value of 371 nm for 3PT (3.34 eV).

This difference is because of an infinite number of nPT length considered in experimental work while our calculation simulated based on limit length of polymer with three rings (3PT). From the data listed in Table 3, it is obvious that when species bounds with 3PT, the λ_{max} values for complexes are blue shifted for SO_3 (-0.225 eV) and HCN (-0.114 eV) and red shifted for H_2O (0.029 eV), NH_3 (0.007eV) and H_2S (0.001 eV) which is due to $\pi \rightarrow \pi^*$ transition. These blue and red shifted values illustrate the sensing aptitude of 3PT towards mentioned species. Moreover, the higher shifting in the case of interaction of SO_3 with 3PT is totally in accordance to its higher value of adsorption energy than other systems which can attribute to appearing new bonds as can be confirmed by the HOMO-LUMO distribution in Fig.2.

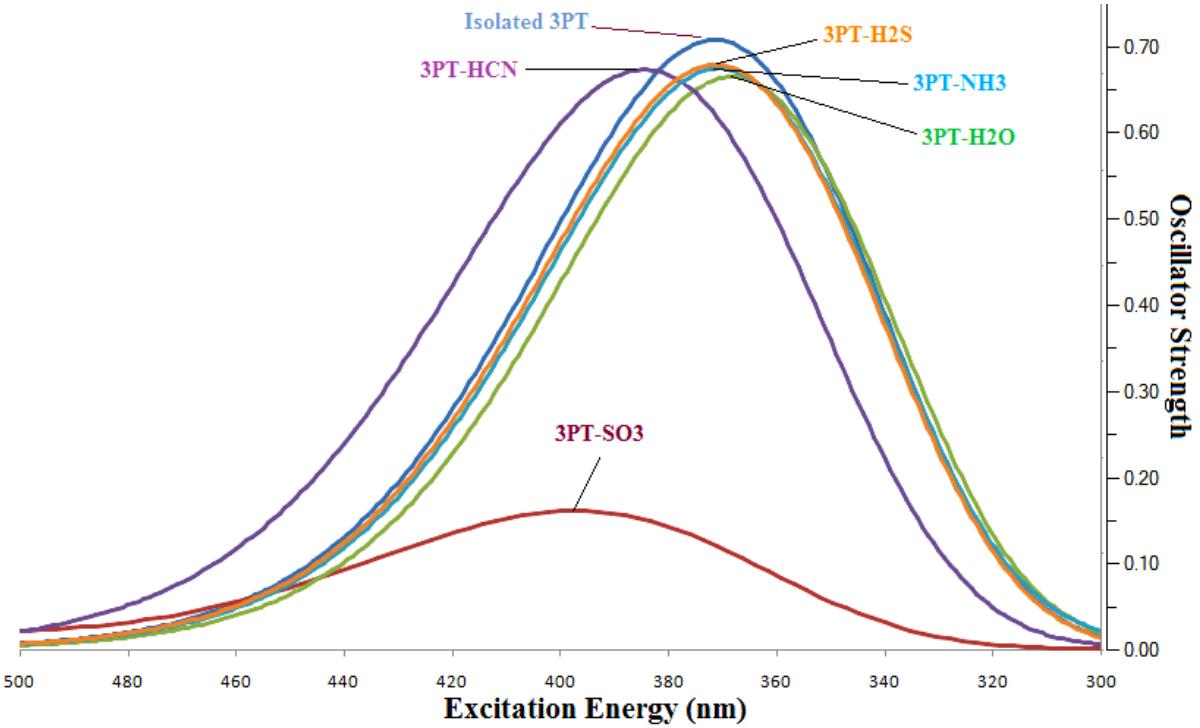

Figure 3. UV-vis spectra of isolated 3PT, 3PT- H_2O, 3PT-SO_3, 3PT-NH_3, 3PT-HCN and 3PT-H_2S

Table 3. UV-vis parameter for different 3PT-X complexes TD-SCF BLYP-D3/6-31+G (d) level of theory

system	λ_{max} (nm)	λ_{max} (eV)	ΔE (eV) λ_{max} shifting	Result
Isolated 3PT	371.46	3.338	-	-
3PT- H_2O	368.29	3.367	+0.029	Red shift
3PT-SO_3	398.22	3.113	-0.225	Blue shift
3PT- NH_3	370.61	3.345	+0.007	Red shift
3PT-HCN	384.51	3.224	-0.114	Blue shift
3PT-H_2S	371.29	3.339	+0.001	Red shift

4. Conclusion

We used DFT method to search on the interaction of H_2O, HCN, NH_3, SO_3, and H_2S with 3PT (as a simple model for polythiophene). To further understanding the electronic properties of 3PT-analytes structures, the charge and orbital analyses were calculated for the isolated 3PT as well as different 3PT-analytes complexes. The type of interaction between mentioned species with 3PT was studied with understanding the HOMO and LUMO energies. Electronic properties simulation such as band gap from the energies of HOMO and LUMO support the sensing ability of 3PT (and actually polythiophene) towards above-mentioned species. UV-vis spectra analysis has been used for all 3PT- analytes as well as isolated 3PT and related spectrums show that the λ_{max} values were red or blue shifted depend on the kind of complex

which are proof of successful interaction between 3PT and mentioned species. All analyses reveal physisorption process for all species upon interaction with 3PT.

Acknowledgments

We highly acknowledge financial support from Islamic Azad University, Qaemshahr Branch, Iran.

References

[1] Chou YM, Chen WH, Liang CC (2009) Substituent effects and photo-physical properties in polythiophene and its derivatives: A PBC-DFT study, Journal of Molecular Structure: THEOCHEM 894: 117–120.

[2] Pesant S, Boulanger P, Coté M, Ernzerhof M, (2008) Ab initio study of ladder-type polymers: Polythiophene and polypyrrole, Chem. Phys. lett 450: 329-334.

[3] Bai H, Shi G (2007) Gas Sensors Based on Conducting Polymers, Sensors 7: 267-307.

[4] Chang JB, Liu V, Subramanian V, Sivula K, Luscombe C, Murphy A, Liu J, Frechet JM (2006) Printable polythiophene gas sensor array for low-cost electronic noses, J. Appl.Phys., 100: 014506.

[5] Shokuhi Rad A, Shadravan A, Soleymani AA, Motaghedi (2015)N, Lewis acid-base surface interaction of some Boron compounds with N-doped graphene; First principles study, Curr. Appl. Phys. 15: 1271-1277.

[6] Shokuhi Rad A., Kashani Razzaghi. O. (2015) Adsorption of Acetyl Halide molecules on the surface of pristine and Al-doped graphene: ab initio study, Appl. Surf. Sci 355: 233–241.

[7] Shokuhi Rad A, Valipour P (2015) Interaction of methanol with some aniline and pyrrole derivatives: DFT calculations, Synthetic Met. 209: 502–511.

[8] Shokuhi Rad A., Nasimi N, Jafari M, Sadeghi Shabestari D, Gerami E (2015) Ab-initio study of interaction of some atmospheric gases (SO_2, NH_3, H_2O, CO, CH_4 and CO_2) with polypyrrole (3PPy) gas sensor: DFT calculations, Sensors Actuat. B 220: 641-651.

[9] Shokuhi Rad A, Zardoost M R., Abedini E, (2015) First-principles study of terpyrrole as a potential hydrogen cyanide sensor: DFT calculations, J Mol. Model 21:273.

[10] Shokuhi Rad A, Valipour P, Gholizade A, Mousavinezhad SE (2015) Interaction of SO_2 and SO_3 on Terthiophene (as a model of polythiophene gas sensor): DFT calculations, Chem. Phys. Lett. 639: 29–35.

[11] Shokuhi Rad A. (2015) Application of polythiophene to methanol vapor detection: an ab initio study, J Mol Model 21:285.

[12] Shokuhi Rad A. (2015) Terthiophene as a model sensor for some atmospheric gases: Theoretical study, Molecular physics, 114:584-591.

[13] Shokuhi Rad A (2015) Al-doped graphene as sensitive nanostructure sensor for some ether molecules: ab-initio study of adsorption. Synthetic Met. 209: 419–425.

[14] Shokuhi Rad A (2015) First principles study of Al-doped graphene as nanostructure adsorbent for NO_2 and N_2O: DFT calculations, Applied Surface Science, 357 (2015) 1217–1224.

[15] Shokuhi Rad A, (2015) Density functional study of Al-doped graphene nanostructure towards adsorption of CO, CO_2 and H_2O, Synthetic Met. 210:171–178.

[16] Shokuhi Rad A, Esfehanian M, Maleki S, Gharati G, (2016) Application of carbon nanostructures towards SO_2 and SO_3 adsorption: a comparison between pristine graphene and N-doped graphene by DFT calculations, J. Sulfur Chem, 37: 176-188.

[17] Shokuhi Rad A (2016) Al-doped graphene as a new nanostructure adsorbent for some halomethane compounds: DFT calculations, Surface Science 645: 6–12.

[18] Shokuhi Rad A, Abedini E (2016) Chemisorption of NO on Pt-decorated graphene as modified nanostructure media: a first principles study, Appl Surf Sci. 360: 1041–1046

[19] Zamoshchik N, Salzner U, Bendikov M (2008) Nature of charge carriers in long doped oligothiophenes: the effect of counterions, J. Phys. Chem. C. 112: 8408–8418.

[20] Patra A, Wijsboom YH, Leitus G, Bendikov M (2011) Tuning the Band Gap of Low-Band-Gap Polyselenophenes and Polythiophenes: The Effect of the Heteroatom , Chem. Mater. 23: 896–906.

[21] Bouzzine SM, Salgado-Morán G, Hamidi M, Bouachrine M, Pacheco AG, Glossman-Mitnik D (2015) DFT study of polythiophene energy band gap and substitution effects, Journal of Chemistry Article ID 296386, http://dx.doi.org/10.1155/2015/296386

[22] Liao F, Toney MF, Subramanian V (2010) Thickness changes in polythiophene gas sensors exposed to vapor, Sensors and Actuators B 148: 74–80.

[23] Sakurai ., Jung HS, Shimanouuchi T, Inoguchi T, Morita,A, Kuboi R, Natsukawa K (2002) Novel array-type gas sensors using conductiong polymers and their performance for gas identification, Sensors and Actuators B 83: 270-275.

[24] Goncalves VC, Nunes BM, Balogh DT, Olivati CA (2010) Detection of volatile organic compounds using a polythiophene derivative, Phys. Status Solidi A. 207: 1756–1759.

[25] Gonçalves VC, Balogh DT (2012) Optical chemical sensors using polythiophene derivatives as active layer for detection of volatile organic compounds, Sensors and Actuators B: Chemical 162: 307-312.

[26] Neese F (2012) The ORCA program system, Wiley Interdiscip. Rev: Comput. Mol. Sci. 2: 73–78.

[27] Grimme S, Antony J , Ehrlich S, Krieg H (2010) A consistent and accurate ab initio parametrization of density functional dispersion correction (DFT-D) for the 94 elements HPu. J Chem Phys., 132: 154104.

[28] Zhao Y, Truhlar DG (2004) Hybrid Meta Density Functional Theory Methods for Thermochemistry, Thermochemical Kinetics, and Noncovalent Interactions: The MPW1B95 and MPWB1K Models and Comparative Assessments for Hydrogen Bonding and van der Waals Interactions, J. Phys. Chem. A, 108:6908.

[29] Peng S, Cho K., Qi P, Dai H (2004) Ab initio study of CNT NO_2 gas sensor, Chem Phys Lett. 387: 271-276.

[30] Tomfohr J K, Otto FS (2002) Complex band structure, decay lengths, and Fermi level alignment in simple molecular electronic systems, Phys. Rev. B **65**: 245105.

[31] Boys SF, Bernardi F (1970) The calculation of small molecular interactions by the differences of separate total energies. Some procedures with reduced errors, Mol. Phys. 19: 553-566.

[32] Diaz A, Crowley J, Bargon J, Gardini GP, Torrance JB, (1981) Electrooxidation of aromatic oligomers and conducting polymers., J. Electroanal. Chem. 121: 355–361.

[33] Chattaraj PK, Giri S (2009) Electrophilicity index within a conceptual DFT framework, Annu. Rep. Prog. Chem., Sect. C: Phys. Chem. 105: 13-39.

[34] ShokuhiRad A, Ayub K (2016) Ni adsorption on $Al_{12}P_{12}$ nano-cage: DFT study**,** Journal of Alloys and Compounds, DOI: 10.1016/j.jallcom.2016.03.175

[35] Guangtao L, Sheshanath B, Tianyu W, Yang Z, Hesun Z, Fuhrhop JR (2003) Angew. Chem. Int. Ed. 42, 3818-3821.